NASA Technical Memorandum 86670

Airborne Astronomy Program
Medium Altitude Missions Branch
Preprint Series 026

Far-Infrared Line Observations of Planetary Nebulae: I. The [O III] Spectrum

Harriet L. Dinerstein, Daniel F. Lester, and Michael W. Werner

February 1985

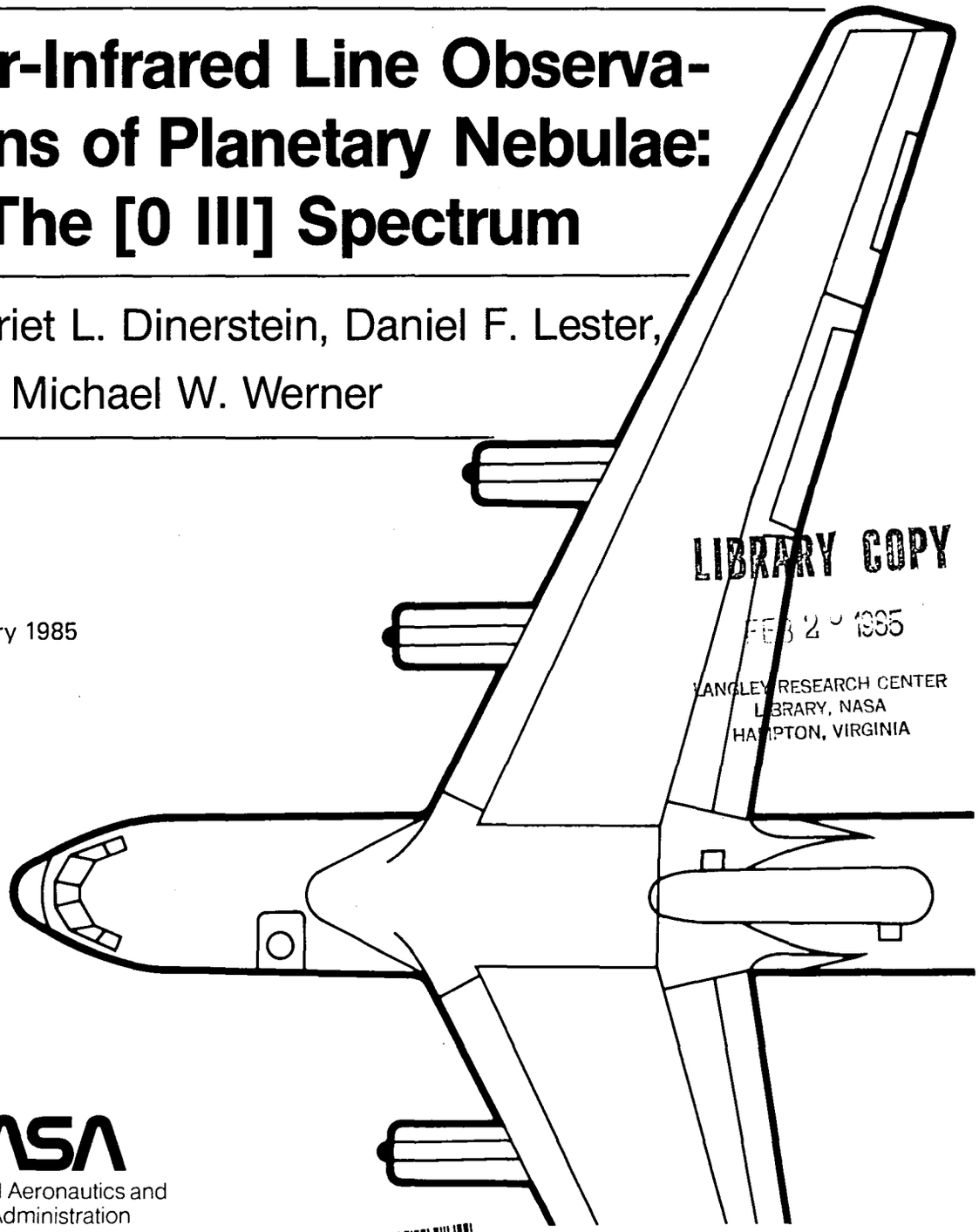

National Aeronautics and Space Administration

NASA Technical Memorandum 86670

Airborne Astronomy Program
Medium Altitude Missions Branch
Preprint Series 026

Far-Infrared Line Observations of Planetary Nebulae: I. The [O III] Spectrum

Harriet L. Dinerstein
Daniel F. Lester, University of Texas at Austin, Austin, Texas
Michael W. Werner, NASA Ames Research Center, Moffett Field, California

National Aeronautics and
Space Administration

Ames Research Center
Moffett Field, California 94035

Ap. J., in press

FAR-INFRARED LINE OBSERVATIONS OF PLANETARY NEBULAE:

I. THE [O III] SPECTRUM

Harriet L. Dinerstein and Daniel F. Lester
University of Texas at Austin

and

Michael W. Werner
NASA-Ames Research Center

ABSTRACT

Observations of the far-infrared fine-structure lines of [O III] have been obtained for six planetary nebulae. The infrared measurements are combined with optical [O III] line fluxes to probe physical conditions in the gas. From the observed line intensity ratios, we obtain a simultaneous solution for electron temperature and density, as well as a means of evaluating the importance of inhomogeneities. Densities determined from the far-infrared [O III] lines agree well with density diagnostics from other ions, indicating a fairly homogeneous density in the emitting gas. Temperatures are determined separately from the [O III] 4363/5007Å and 5007Å/52μm intensity ratios and compared. Systematically higher values are derived from the former ratio, which is expected from a nebula which is not isothermal. Allowance for the presence of temperature variations within these nebulae raises their derived oxygen abundances, which may allow us to reconcile nebular oxygen abundance determinations with the solar value.

Subject headings: nebulae:planetary - nebulae:abundances - infrared:spectra

I. INTRODUCTION

The brightest emission lines in the optical spectra of most planetary nebulae are the forbidden [O III] lines at 4959 A and 5007 A. The same ion gives rise to fine-structure lines from the ground ^3P term at 51.7 and 88.4 μm. The far-infrared lines have been observed in a number of luminous, obscured H II regions from NASA's Kuiper Airborne Observatory (Ward et al. 1975; Melnick et al. 1979; Moorwood et al. 1980; Watson et al. 1981). In this paper, we present the first comprehensive set of emission line measurements for the ground configuration of [O III], for several planetary nebulae. These measurements are used to demonstrate new techniques for studying physical conditions in ionized nebulae. These lines are well suited to the study of nebular conditions since O^{++} occupies a large fraction of the volume of ionized gas in most planetary nebulae.

In general, the emissivities of the far-infrared fine-structure lines have very different dependences on the physical conditions as compared to the optical lines (Simpson 1975, Watson and Storey 1980). The infrared line strengths are insensitive to the electron temperature due to the very small energy of their upper levels, whereas the optical lines arise from higher-lying levels and are very sensitive to temperature; indeed, the ratio between the $^1S_0$-$^1D_2$ (4363 A) and $^1D_2$-$^3P_{1,2}$ (4959, 5007 A) [O III] lines is a primary diagnostic of electron temperature in nebulae (see Figure 1). On the other hand, the critical electron densities for collisional de-excitation to dominate radiative decay are relatively low for the [OIII] infrared lines, so that their intensity ratio is a good density indicator in the regime n_e-10^2-$10^4 cm^{-3}$, which is appropriate for most planetary nebulae. Comparisons of measured infrared and optical line

fluxes can be used to solve simultaneously for electron temperature and density (Dinerstein 1983). Further, when lines arising from among all three terms are measured, it should be possible in principle to evaluate the magnitude of variations or fluctuations of temperature and density within the O^{++} region. The presence of such variations is of interest, because when taken into account, they have a significant effect on the derived ionic abundances (Rubin 1969; Peimbert and Costero 1969).

In 1981, we began a program of observing the far-infrared lines of [O III] (as well as [N III] 57.3 μm) in bright, moderately-extended planetary nebulae, in order to study their physical conditions and ionic abundances. (This project was done in parallel with a survey of N/O abundances in galactic H II regions; the H II region results are presented in Lester et al. 1983 and Lester et al. 1984a). Measurements of the [O III] 88 μm line in four planetary nebulae and a preliminary analysis of temperature and density through comparison with optical line intensities were presented by Dinerstein (1983). The current paper presents new and more complete [O III] measurements for six planetary nebulae, with both infrared lines measured for four of these. Physical conditions inferred from the line ratios are discussed. Measurements of [N III] 57 μm in several planetary nebulae and a discussion of the ionic abundance ratio N^{++}/O^{++} will appear in a separate paper (Dinerstein, Lester, and Werner, in preparation).

II. OBSERVATIONS

a) Selection Criteria

The observed nebulae are listed in Table 1. They were selected according to several criteria: 1) bright hydrogen line or radio continuum emission; 2)

moderate to high degree of ionization to ensure a large fraction O^{++}/O; and 3) moderate electron densities ($n_e \leq 10^4$ cm^{-3}). The last is important because at very high densities the density-normalized emissivities of the infrared fine-structure lines are collisionally suppressed (see Sec. IIIa); for example, these lines have not been seen in the small dense nebula NGC 7027 despite its large emission measure (Melnick et al. 1981; Watson et al. 1981). The only planetary nebula in which an [O III] fine-structure line flux had been measured previously was NGC 6543, detected by Watson et al. (1981). Evidence for the 52 μm line was also seen in a low-resolution spectrum of NGC 6543 obtained by Moseley and Silverberg (1981).[1] Since our study was in part motivated by an interest in measuring nitrogen overabundances and variations among planetary nebulae, we included several objects believed to have very large nitrogen enhancements (NGC 2440, 6302, and 6445).

b) Far-Infrared Line Observations

The far-infrared line measurements were made with the 91 cm telescope of NASA's Kuiper Airborne Observatory (KAO) during four flight series: June 1981,

---

[1]NGC 6543 was the first planetary nebula for which both far-infrared [O III] lines were measured, in June 1981. As pointed out by Czyzak, Aller, and Kaler (1968), it was also the first planetary observed spectroscopically in the optical, and the celestial object in which the green [O III] lines were discovered, by Huggins (1864). Furthermore, NGC 6543 was also the first planetary nebula whose ultraviolet spectrum was observed (Pottasch 1984), more than a century after the first inspection of its optical spectrum.

February 1982, July 1982, and May 1983. The last of these was part of the Southern Hemisphere expedition of the KAO, sponsored jointly by the US and Australian governments, and enabled us to complete the measurements on several southern nebulae. The instrument was the tandem Fabry-Perot spectrometer described by Storey, Watson, and Townes (1980) and Watson (1982). The beam diameter was between 40" and 50" FWHM, depending on the flight series. In all cases, the beam was larger than the bright nebular cores (Table 1) so that the infrared measurements represent integrated line fluxes. The chopper throw was typically 4' in azimuth. The nebular cores or central stars were generally visible in the KAO tracker camera, so it was possible to guide directly on the object. Centering errors were approximately 5-10", due to the small plate scale of the tracking camera.

The observations were made with spectral resolution of $\lambda/\Delta\lambda$ = 1000-3000, which was not, in most cases, high enough to spectrally resolve the emission lines, since the intrinsic linewidths are only about 30-40 km s^{-1} (e.g. Welty 1983). About 5-10 resolution elements were scanned during each line measurement, covering a wavelength range of 0.1-0.5 μm. At this resolution, the continuum emission from dust in the planetary nebulae (Moseley 1980) is very weak, so that the equivalent widths are very large, unlike the situation for many galactic H II regions. Of the observed nebulae, continuum was detected only in NGC 6302. The water vapor column density was typically 2-15 μm although no correction for terrestrial atmospheric opacity was made since, at these values, the scanned passbands do not contain any significant atmospheric absorption lines.

Integration times on the planetary nebulae were typically 15-40 minutes,

and in general a signal-to-noise ratio of 10 or better was achieved. Several representative spectra are shown in Figure 2. The spectra were oversampled by large factors during data-taking, and were later binned as displayed in the figure. The lines were then fitted with Lorentzian profiles appropriate to the instrumental response, as shown, and the fluxes were derived from the fitted profiles.

Since the purpose of this study is to make a detailed comparison of the absolute infrared and optical line fluxes, accurate absolute flux calibration is essential. Our primary flux calibrations were the NASA-Ames spectroscopic measurements of Simpson et al. (1981) for Mars and Haas et al. (1982) for Saturn. The latter calibration takes into account the different brightness temperatures of the rings and disk and the obscuration of the disk by the rings as a function of ring inclination. The 52 μm line fluxes (except in NGC 6302) were calibrated directly against either Mars or Saturn, by observing nebula and planet on the same flight; two independent measurements were made for NGC 3242. The 88 μm line fluxes were derived using galactic far-infrared sources of known colors as secondary calibrators and adjusting their absolute flux levels, if necessary, to bring them onto the system defined by the primary calibrators described above. The secondary calibrators included G333.6-0.2 (Hyland et al. 1980), NGC 7538 (Werner et al. 1976), Sgr A (Gatley et al. 1977), and G25.4-0.2 (Lester et al. 1984b).

We can compare our fluxes for these objects, derived using the NASA-Ames calibrations of the planets, with previously measured and published values. The comparison indicates a high degree of consistency with the older measurements. For example, at 52 μm, our flux for the central arcminute of Sgr A is within 5%

of that derived by Gatley et al. (1977), whose flux calibration is based on Pioneer 10 measurements of Jupiter. For G333.6-0.2, our measurement is 15% lower than that derived by Hyland et al. (1980), once their fluxes (calibrated according to the Yerkes broad-band calibration of Saturn) are corrected by 30% to bring them onto the Ames system. The latter discrepancy in the Saturnian flux is attributed to the variation of brightness temperature with ring inclination that is explicitly accounted for in the Ames calibration. When reduced to a common calibration pedigree, previously published continuum measurements of other objects show consistency with our measurements on a similar (~ 15%) level. The accuracy of our absolute calibration is determined by any systematic errors in the Ames calibration. For future measurements, the IRAS catalog will provide an independent, internally consistent set of flux calibrators.

In a few cases, it was necessary to make a small correction in order to account for the difference in instrument response to sources of different sizes. Since the nominal beam size is not much larger than the Airy disk of the telescope, the beam profile is strongly affected by diffraction, and the beam shape is approximately Gaussian. As a result, measurements of extended sources are biased toward the central portion of the beam, in contrast to the optical measurements, for which the beam is cylindrical (flat). In most cases, the calibrator (e.g. Saturn or an H II region) subtended a similar solid angle as the planetary nebulae, so the differential effect was negligible. The exceptions are the 52 μm measurements of NGC 6543 and NGC 6826 calibrated by Mars, which is significantly smaller than these nebulae (see Table 1). We compared the response of a Gaussian beam to a very small source with that to cylindrical sources of various radii, representing the planetary nebula shells,

and derived corrections to the line fluxes of 4% for NGC 6543 and 6% for NGC 6826, which have been applied to the data.

The infrared line fluxes are given in columns 2 and 3 of Table 2. The quoted uncertainties represent the total uncertainty in the line fluxes arising from both flux calibration consistency and statistical errors. In almost all cases, the dominant source of error was uncertainty in the flux calibration, which we estimated by comparing observations of different secondary flux calibrators during each flight series. In addition, the two independent measurements of [O III] 52 μm in NGC 3242 differed by only 8%. The 52 μm lines in NGC 2440, NGC 3242, NGC 6543, and NGC 6826 were measured to better than 15% accuracy. Accurate 52 μm intensities are particularly critical to our analysis because they are used in direct combination with absolute optical intensities.

c) Optical Line Observations

In order to compare the far-infrared and optical line intensities, one must use integrated fluxes, because of the low spatial resolution of the infrared measurements. While many optical studies have been made of the planetary nebulae observed here (e.g. Aller and Czyzak 1983 and references therein), in most cases such studies have used apertures much smaller than the regions of bright emission and thus these line ratios are not necessarily representative of the ratios in integrated light. An exception to this is the large-beam (34" diameter) study of optical [O III] line ratios by Bohuski, Dufour, and Osterbrock (1974), who observed NGC 6543 and NGC 6826. To supplement the available optical data, we used the Lick Observatory Crossley reflector to measure absolute integrated line intensities for NGC 6445, NGC 6543, and NGC 6826 in August 1981. These measurements were made with the Wampler sequential

programmable scanner (Wampler 1966). Observations of [O III] 5007 A and Hβ were made through 45" and 70" diameter apertures, with spectral resolution adequate to resolve these lines and with no vignetting of the entrance aperture. The data were calibrated using the standard stars of Hayes (1970) revised according to the calibration of Hayes and Latham (1975). Extinction constants were calculated for each night from observations of standard stars at different airmasses.

For the other three nebulae, 5007 A fluxes were scaled from published large-aperture photoelectric observations. Kaler (1976) measured the integrated [O III] 4959 A fluxes from NGC 2440 and NGC 3242, which are related to the 5007 A fluxes by the ratio of transition probabilities. Danziger, Frogel, and Persson (1973) observed NGC 6302 in a 17" x 34" beam which, although not large enough to give integrated fluxes, should yield line ratios which are representative of the integrated light; this data was combined with indicators of the hydrogen emission measure to reconstruct an integrated 5007 A flux.

The 4363/5007A ratio is an important indicator of nebular conditions that we will use in our analysis. We again prefer to use values measured in integrated light. As mentioned above, Bohuski, Dufour, and Osterbrock present direct measurement of the integrated ratios for NGC 6543 and NGC 6826; Danziger, Frogel, and Persson give a measured ratio for NGC 6302 in a large beam. For the other nebulae, it was necessary to use measurements in the literature that were made in a variety of beam sizes; references to these are given at the bottom of Table 2.

The optical fluxes and flux ratios were corrected for extinction using the

relation of Miller and Mathews (1972) and the values for the Hβ extinction parameter, $c = \log \{F_{true}(H\beta)/F_{obs}(H\beta)\}$, listed in Table 1. The extinction-corrected values in Table 2 were computed as follows:

$$F_{5007} = (F_{5007})_{obs}\, 10^{0.97c} \qquad (1)$$

and

$$\log(F_{5007}/F_{4363}) = \log(F_{5007}/F_{4363})_{obs} - 0.18c \qquad (2)$$

where the subscripted values are the observed and the unsubscripted values are the extinction-corrected quantities. These corrections are negligible for NGC 3242 and NGC 6826, and small (less than 0.1 dex in $\log F_{5007}/F_{4363}$) for NGC 2440 and NGC 6543. The largest corrections are for the southern nebulae NGC 6302 and NGC 6445, which have large extinctions probably varying across each nebula. These two nebulae were observed primarily in order to study their reported nitrogen overabundances, which can be studied directly from the ratio of the far-infrared lines and is not sensitive to extinction. Only one of the far-infrared [O III] lines was measured for each of these nebulae, and a more limited analysis of the [O III] ratios was carried out than for the other four objects.

The extinction-corrected integrated optical fluxes and ratios are listed in Tables 1 and 2. Based on agreement in the literature among various measurements of integrated line fluxes and extinctions, we have assigned an uncertainty of 10% to the 5007 A fluxes in NGC 3242 and NGC 6826, which have negligible or zero

extinction, 15% uncertainty for NGC 2440 and NGC 6543, and 25% uncertainty for NGC 6302 and NGC 6445. The uncertainties in the 4363/5007A ratio are harder to evaluate, since the measurements do not all represent direct integrated ratios, but are probably substantially smaller than the errors in the 5007 A fluxes.

d) Outer Halos

Several of the observed planetary nebulae are known to have extended faint outer shells (e.g. Kaler 1974). That of NGC 6826 can be seen quite clearly on the red print of the Palomar Sky Survey. Photographs of the outer shells of NGC 6543 and 6826 were taken by Millikan (1974); that of NGC 6543 shows clumpy structure. NGC 3242 has multiple-shell structure, including a very large faint outer shell (Bond 1981), and NGC 2440 is also known to be surrounded by faint extended emission in long-exposure photographs (Minkowski 1964). The outer diameters of these shells are several arc minutes, and they are generally fairly circular. NGC 6302 is a special case; although optical photographs show an extended biconical "butterfly" pattern, infrared and radio mapping has shown that most of the material is contained in a central toroid possibly confining a biconical outflow (see Lester and Dinerstein 1984).

The possible contribution of these faint halos to the infrared line fluxes is of some concern since their low densities and hence lack of collisional deexcitation might make them relatively brighter in the infrared lines. In order to assess the contribution of these outer shells to the large-beam flux measurements, we traced the intensity profiles of [O III] 5007 A across NGC 6543 and NGC 6826 and compared them with similar traces across bright stars. From these measurements it was clear that the contrast of core to halo is very high, and that nearly all of the optical [O III] emission arises in the inner 40".

The optical surface brightness of the halo is everywhere less than 1% that of the central regions. Thus, even if a high density in the nebular core suppresses the infrared line emission relative to the emissivity from the low-density halo (by a factor of about 5 for log n_e = 4.0 as in NGC 6543), the halo should still contribute $\lesssim$ 15% of the infrared flux. In addition, we made a measurement at 88 μm in the halo of NGC 6543, centered on a comparatively bright knot (Millikan 1974) about 40" east of the central star. No line emission was detected, although our 3σ upper limit of $< 4 \times 10^{-18}$ W cm^{-2} per beam is only about 30% of the peak, a less stringent limit than that derived from the optical measurements. We conclude that there is no evidence for an important contribution to the infrared line fluxes from the nebular halos, even in the case of NGC 6543, where it might have the largest expected effect because of the high density of the nebular core and the relatively bright halo. The density structure of the inner regions of the observed nebulae will be discussed in Sec. IV.

III. ANALYSIS

a) Line Emissivities

The volume emissivities for the [O III] lines were determined using a 5-level equilibrium code including collisional excitation and deexcitation by thermalized electrons, and spontaneous radiative decay. Proton impact excitation is negligible at these temperatures, and has been ignored. The collision strengths are from the recent calculations by Aggarwal, Baluja, and Tully (1982) and Aggarwal (1983), and the transition probabilities are from Baluja and Doyle (1981). The temperature-dependence of the collision strengths was included explicitly in the calculations. The new collision strengths for

the far-infrared lines are about 30% higher than the values of Saraph, Seaton, and Shemming (1969), which were used in the analyses of Dinerstein (1983) and Lester et al. (1983). The new collision strengths for the optical transitions are slightly lower than the previously used values of Eissner and Seaton (1974).

The derived 52 μm emissivity and 52/88μm emissivity ratio are shown as a function of temperature and density in Figure 3. The largest effect of the new emissivities is on the ratio of 5007Å/52 μm, which yields a higher temperature for a given observed ratio than one would derive using the older values. The relation between the 52/88μm emissivity ratio and the density shows less change because the collision strengths of both infrared lines increased by about the same amount although the individual critical densities are lower.

b) The Temperature-Density Plane

By measuring the far-infrared as well as the optical forbidden transitions, we can build a uniquely complete picture of the excitation of the O^{++} ion. Due to the different dependences of each transition on the density and temperature, we can construct line ratios which will allow us to determine the temperature and density simultaneously and nearly independently. This is, in principle, more physically justifiable than using the intersection of density and temperature indicators provided by ions of widely differing ionization potential, which has been the usual procedure (e.g. Barker 1978; Aller and Czyzak 1983). For example, [O II] often provides the main density indicator for nebular analyses, while the temperature is determined from [O III]. We initially assume homogeneity in n_e and T_e, although, as we will see below, our measurements will allow us to test this assumption.

In practice, we will plot each nebula as a point in a line-ratio plane, corresponding to a unique pair of values of T_e and n_e. It is useful to take two line ratios which separate the dependences on temperature and density as much as possible. The ratio of 4363/5007A, as discussed above, depends essentially only on temperature, while 52/88μm depends chiefly on density. The ratio of 5007 A to the far-infrared lines depends on both temperature and density. Results for four planetary nebulae in which the 88 μm line of [O III] had been measured were presented by Dinerstein (1983), using 4363/5007A as the temperature axis and 5007A/88μm as a density indicator.

Use of the 4363 A line to determine the mean electron temperature of a nebula has been called into question. The strong temperature sensitivity of the 4363 A line means that the hottest gas present contributes disproportionately and enhances the observed 4363/5007A ratio. Thus, the presence of even a small amount of very hot gas, for example material shocked by a wind from the central star, could raise the apparent temperature significantly. In the presence of variations in temperature, the 4363/5007A ratio will be weighted by the higher-temperature material; this effect will be discussed quantitatively below. Enhancement of the 4363 A line due to radiative cascading from higher levels is probably not an important effect (Shields, Dalgarno, and Sternberg 1983).

The ratio of 5007 A to the infrared lines offers another way to measure the temperature. With the set of line fluxes in Table 2, we can now locate the nebulae in a temperature-density diagram which does not involve the 4363 A line. We choose to use 5007A/52 μm as the temperature indicator because the relatively high critical density of the 52 μm line minimizes any residual density dependence. In Figure 4, the four nebulae for which we have a complete set of

measurements are shown plotted in this alternate line-ratio plane. The error bars correspond to the uncertainties in the fluxes as given in Table 2. The loci of the line ratios are shown for temperatures from 5000 to 20,000 K and densities from log n_e = 2.0 to 4.5 (cm^{-3}). The derived temperatures and densities are compared with values determined by other methods in Table 3 and are discussed in the following section.

IV. RESULTS

a) Densities

The far-infrared [O III] lines give us a direct way of measuring the local gas density in the O^{++} zone, which contains the bulk of the ionized gas in most planetary nebulae. Optical density indicators generally arise from trace ions, and thus sample a small and not necessarily representative region of the nebula. Table 3 compares the densities determined from our [O III] measurements with values derived from the optical [O II] line ratios. The nebulae are relatively bright and well-studied in the optical; the scatter among published determinations implies an uncertainty of about ±0.2 dex in log n_e(O II). The estimated errors in log n_e(O III) as determined from the far-infrared lines are also about 0.2 dex, as seen from Table 2 and Figure 4. The agreement between the [O III] and [O II] densities is striking. By contrast, some previous studies (e.g. Aller and Epps 1976) found systematically different densities from different ions; for example, they found that the red [SII] lines generally indicated higher densities than the [OII] lines. Although such an effect is not strongly indicated by more recent measurements (Aller and Czyzak 1983), we may reconcile it with our result if much of the [S II] emission arises from denser, partially ionized inclusions, while the more completely ionized material is

relatively homogeneous in density.

In two nebulae, NGC 6302 and NGC 6445, only one of the far-infrared [O III] lines was observed, so the 52/88μm ratio is not available as a density indicator. However, we can still solve for temperature and density using the available line ratios. We determine the temperature from the 4363/5007A ratio and derive an [O III] density from the ratio of 5007 A to the measured infrared line, 52 μm in the case of NGC 6302 and 88 μm for NGC 6445. The [O III] density is very high in the structurally complex object NGC 6302, whose morphology was studied by Lester and Dinerstein (1984). The 52 μm line presumably comes primarily from the dense central toroidal or disk structure seen in the infrared and radio, which contains most of the ionized gas but is largely hidden in the optical by local extinction. The somewhat lower [O II] density, measured from lines in the blue, may simply reflect a lower density in the biconical lobes visible on either side of this central structure. For NGC 6445, also a structurally complex and heavily obscured nebula, we have only an upper limit on the 88 μm flux and hence a lower limit on the density, which is consistent with the [O II] value.

Our conclusion that the densities in the O^+ and O^{++} regions are the same in each nebula within a factor of two must be considered in view of two possibly important observational biases, both of which would have the effect of making the apparent [O III] densities lower than the [O II] values. First, the far-infrared observations are made in a large beam which integrates over the nebula. The optical line ratio observations, on the other hand, are mostly made with small apertures, typically a few arc seconds across, which are usually set at positions of high surface brightness. Thus, positions of higher than average

density may be selectively sampled by the optical measurements. A more fundamental effect arises from the expected behavior of any density-sensitive emission line or line ratio. Because their density-normalized emissivities decrease rapidly at high densities (see Fig. 3), the far-infrared [O III] line emission can be dominated by regions of low density, if a large volume of low-density gas is present. On the other hand, the low-density gas will be a relatively less important contributor to emission in the optical [O II] lines, which have higher critical densities. Therefore, systematically higher [O II] densities are a natural consequence of the dependences of the line emissivities in the presence of nebular density inhomogeneities, independent of any special ionization structure. Both of these local densities will, in general, be different from the globally-averaged rms density $\langle n_e^2 \rangle^{1/2}$ determined from the hydrogen emission measure, and from densities determined from other ionic lines with different critical densities.

The good agreement between the [O III] and [O II] densities suggests that these biases are not important in the planetary nebulae, unless they conspire to negate an ionization effect. We prefer the simpler explanation, that these nebulae are relatively homogeneous in density. Quantifying this conclusion requires a model for the spectrum of density variations. One approximation is that of small fluctuations around a mean density (Peimbert 1971); another is a two-zone model (e.g. Moorwood et al. 1980). The real situation is likely to be more complex, requiring the use of a continuous function describing the fraction of gas as a function of density (e.g. the sinusoidal characterization of Mihalszki and Ferland 1983). Using integrated fluxes, we are not able to separate angular density variations from clumping along the line of sight. A fuller understanding of the density structure of planetary nebulae will probably

come from combining spectroscopic studies with two-dimensional information, such as well-calibrated high-resolution radio maps (Bignell 1983), in which the density spectrum at spatial scales as small as ~ 100 A.U. can be quantitatively probed.

b) Comparison of Temperature Indicators

For a nebula which is not isothermal, the emission in any line will be weighted by its temperature dependence and will come preferentially from the region where the emissivity is highest. Likewise, any temperature sensitive ratio of lines or line-to-continuum emission will be weighted according to the particular temperature dependences. A formal treatment of this behavior has been developed by Peimbert (1967) and Rubin (1969). These authors parameterized the amplitude of temperature inhomogeneities by a mean temperature T_0 and a temperature fluctuation parameter t^2, in terms of which the line emissivities and deduced temperatures can be easily expressed (see Appendix). For example, recombination line emission has a inverse dependence on T and therefore, in nonisothermal nebulae, it is weighted to regions of low temperature. Optical forbidden lines, on the other hand, are weighted proportionately to various positive powers of temperature. In principle, if more than one temperature-sensitive ratio is measured for a nebula, one can measure both T_0 and t^2. This allows a correction to be made for the presence of these variations when calculating the ionic abundances.

In the case of [O III], the 4363/5007 A ratio is not only a very sensitive temperature indicator, as discussed above, but the temperature inferred from it will exceed the mean temperature by an amount determined by the amplitude of the temperature variations. For four planetary nebulae, we now have the additional

temperature-sensitive [O III] ratio 5007Å/52μm. Using the temperature fluctuation approach (Appendix), we find that, even in the presence of large fluctuations, the ratio 5007Å/52μm yields a temperature which should be close to the mean temperature T_0. For temperatures below about 10,000 K, T(5007Å/52μm) will be slightly larger than T_0, while for higher temperatures, it will be slightly smaller. (This last effect is a consequence of the increasingly important population of the ^1S level, from which 4363Å arises.) Since $T(5007Å/52\mu m) \sim T_0$ and $T(4363/5007Å) \sim T_0(1 + 3\ t^2)$ (see Appendix), the latter value should always be larger than the former in a non-isothermal nebula, if this is the only factor affecting the line ratios.

From Table 3, it can be seen that the temperatures inferred from the 4363/5007Å ratios are systematically higher than those inferred from the 5007Å/52μm ratios. The differences are about 1000 K for NGC 2440 and NGC 6826, 2000 K for NGC 3242, and 3000 K for NGC 6543. The sign of the difference is such that it can be naturally accounted for if temperature variations are present. The corresponding values of t^2 are given in the last column. It is apparent that a value of $t^2 \sim .04$ is representative of this group of nebulae (excluding NGC 6543). This is similar to the value $t^2 = .035$ that was adopted by Torres-Peimbert and Peimbert (1977) in their study of planetary nebulae. While the observational uncertainties are somewhat larger for NGC 6543 and NGC 6826, which were observed early in the program, they actually translate into smaller uncertainties in temperature because of the more sensitive temperature dependence and hence wider spacing of the grid lines (see Figure 4) at lower temperatures.

We must consider whether there are factors other than real temperature

variations which could lead to such a systematic effect in the line ratios. One possible source of systematic effects lies in the atomic parameters used in the analysis: collision strengths and transition probabilities. However, because of its astrophysical importance, O^{++} is one of the best-studied ions. The recent detailed calculations of the [O III] parameters which we use are estimated to be accurate to 10% or better by Mendoza (1983). This estimate is supported by the good agreement between independent calculations of the A-values by Nussbaumer and Storey (1981) and Baluja and Doyle (1981). Differences of this order have negligible effects on the inferred nebular conditions.

A second possible source of systematic error is the correction for extinction. The 5007Å/52μm line ratio and the temperature inferred from it are more sensitive to the adopted extinction value than is the case for 4363/5007Å, so underestimates of the extinction could lead to systematic differences of this kind. However, the extinction values towards the observed nebulae are accurately known, and in two of the four cases, nearly zero. In order to force the two temperature indicators into agreement, the extinction at Hβ would have to be about 60% larger than our adopted values ($\Delta c = +0.2$), which we consider to be very unlikely.

A final source of error is the flux calibration. While the relative fluxes of the infrared lines are not seriously affected by absolute flux calibration errors, the more tenuous connection between visual and far-infrared flux calibrators must be considered as a potential source of error in inferred temperature. In Section IIb, the size of statistical calibration errors was estimated, but we assumed that the standard fluxes themselves (of Mars and Saturn) were error-free. Simpson et al. (1981) and Haas et al. (1982) have

tried to assess this error, and find it unlikely to be greater than 10%.

We consider it improbable that errors in the absolute flux calibration, coupled with the statistical errors in the line fluxes, could manifest themselves as a value of t^2 of the order that we measure. In order to produce t^2 - 0.04 in NGC 3242 and NGC 6826, such an error would have to change the measured 5007 A/52 μm flux ratio by 0.2 - 0.3 dex. We conclude that the observed systematic temperature differences are due to real temperature variations within the nebulae.

Other attempts have been made to look for evidence of temperature variations in the observed nebulae. Shields et al. (1981) measured an O III] line from a different configuration at 1663 A in NGC 2440 and derived the same value from its ratio to 5007 Å as the 4363/5007A temperature. Since temperature variations should lead to an apparently higher temperature using the 1663 A line than using 4363 A because of its larger excitation energy, this appears to rule out the presence of significant fluctuations. However, the UV lines are subject to a large extinction correction for this object, and were measured in a different aperture than the optical lines, so the corrections made for these effects could introduce additional uncertainties. It is also the case that the value of t^2 which we derive from the optical and infrared lines in NGC 2440 is small, t^2 = .025, and due to the crowding of the grid lines at high temperatures (Figure 4), t^2 = 0 is not excluded for this nebula. (The last is not true for the other three nebulae in which t^2 is derived.)

Barker (1979) studied 8 nebulae and compared temperatures derived from forbidden-line and recombination emission. His study included two of our program nebulae, NGC 3242 and NGC 6543. Barker concluded that, in general,

there was no evidence for temperature fluctuations, but the quoted uncertainties in his temperature determinations are sufficiently large that they do not appear to be in conflict with our results. In fact, his observations of NGC 3242 and NGC 6543 appear to indicate [O III] 4363/5007A temperatures that are higher than the Balmer continuum temperatures, for those positions where both quantities are well-determined, although the uncertainties in the latter values are as large as the difference between the two values (1000-2000 K).

Reay and Worswick (1982) constructed temperature maps by combining isophotal intensity contours of 4363 A and 5007 A line emission. They find a nearly uniform temperature of about 11,000 K for NGC 3242, and some evidence that the temperature rises towards the edges of NGC 6543 and NGC 6826, but no clear evidence for small-scale fluctuations. As they point out, however, the use of an independent temperature indicator with a different functional dependence is necessary in order to realistically sample the range of temperatures, as we have done in integrated light.

c) Implications for the Oxygen Abundance

Nebular oxygen abundances are generally considered to be the best-determined of any element heavier than helium. This is the case because the two most important ions, O^{+} and O^{++}, are easily observed in the optical spectral region, and because a temperature can be measured using the [O III] 4363/5007A line ratio, allowing correction for the temperature-dependence of the emissivities. For most other elements, substantial corrections must be made in order to allow for unobserved ions, a procedure which requires assumptions about the ionization structure, and hence introduces a model dependence into the derived abundances. For oxygen, however, direct determinations can be made for

large numbers of planetary nebulae, making it possible to look for real variations in abundance (Kaler 1980). A related but more difficult issue is how the nebular emission line abundances compare with stellar abundances measured from absorption-line studies, which we will discuss below.

The main source of uncertainty in optical nebular abundance determinations results from the need to account properly for the possible presence of temperature inhomogeneities ($t^2 > 0$). In general, allowance for variations in the temperature within the ionized region results in higher derived abundances, as shown by Rubin (1969) and Peimbert and Costero (1969). Most recent nebular abundance analyses have not included a correction for internal temperature fluctuations; that is, they assume $t^2 = 0$. This results in an average oxygen abundance for planetary nebulae of log(O/H) + 12 = 8.64 (Aller and Czyzak 1983). If we adopt this procedure, assuming T_e = T(4363/5007Å) and $t^2 = 0$, the oxygen abundances we derive for the four fully analyzed planetaries studied here are close to this value, all lying in the range 8.6-8.7. (Most of the oxygen in these nebulae is in the O^{++} ion, but we have included O^{+}, and the higher ionization stages in NGC 2440 and NGC 3242 as given by Shields et al. 1981 and Aller and Czyzak 1983.) These values can be compared with the solar abundance of 8.92 ± 0.10 (Lambert 1978). That the nebular abundances are about a factor of two lower than the solar value is surprising since most planetary nebulae arise from a solar-type or possibly younger stellar population.

When the oxygen abundances are corrected for temperature fluctuations by increasing the assumed value of t^2 from 0 to .04 and using T_o = T (5007Å/52 μm), the derived values increase by about 0.2 dex near 10,000 K (see, for example, Torres-Peimbert and Peimbert 1977). For a given value of t^2, the effect is

larger at lower temperatures and smaller at higher temperatures. This change would bring the nebular abundances into better agreement with the solar value, within 0.1 dex for NGC 3242 and NGC 6826. The abundance in NGC 2440 increases by only a small amount because only 40% of the oxygen is in O^{++} in this extremely highly ionized nebula and we have not attempted to correct the other ionic stages for temperature variations. The correction for NGC 6543 actually raises the abundance to above the solar value (nearly a factor of three higher); however, the very filamentary and clumpy nature of this nebula and the large variations in physical parameters implied by the high derived value of t^2 (see Table 3) suggests that the approximation of small fluctuations around a mean temperature value may be breaking down. It is possible that the relatively strong wind from the central star of NGC 6543 (Perinotto 1983 and references therein) has impacted the structure of the nebula so that parameterization of the temperature by a mean value and rms fluctuation index is inappropriate.

Our study has shown that there are significant temperature variations within the O^{++} regions in planetary nebulae. Since accounting for the variations always increases the inferred abundances, the corrected abundances are generally closer to the solar value. Thus, the current factor of two discrepancy between the stellar and nebular abundance scales may be a systematic effect due to the failure to correct nebular values for inhomogeneities in the physical conditions within the ionized gas. Further studies which compare several transitions of a single ion, as we have done for the optical and infrared lines of [O III], have the potential of better defining the magnitude and nature of these variations, and therefore improving the accuracy of the absolute abundance determinations.

V. SUMMARY

We have measured far-infrared fine-structure lines of [O III] at 52 μm and 88 μm in six planetary nebulae, and obtained for the first time a complete line intensity spectrum connecting all levels in the ground term of [O III] for four nebulae. The physical conditions in the O^{++} zone have been explored by utilizing the temperature and density dependences of the various line emissivities.

We find that:

1) The observed nebulae represent a wide range of temperatures and densities;

2) The [O III] densities are similar to those measured from the [O II] line emission (within 0.2 dex) indicating that the density is not correlated with ionization state;

3) Temperatures derived from the [O III] 4363/5007 A ratio are systematically higher than those derived from the 5007A/52μm intensity ratio, as expected if the nebulae are not isothermal. The differences in the inferred temperatures are about 1000-2000 K, and correspond to an average value of .04 for the temperature fluctuation parameter t^2;

4) Correction of the derived oxygen abundances of the planetary nebulae for the indicated temperature variations increases the nebular values by about 0.2 dex, bringing them into closer agreement with the solar abundance.

ACKNOWLEDGEMENTS

The authors are grateful to Drs. M. Crawford, R. Genzel, J.W.V. Storey, C. H. Townes, and D. M. Watson for the use of their spectrometer and for their generous and extensive assistance in obtaining the far-infrared observations. This project was made possible through the guest observer program on the NASA Kuiper Airborne Observatory. We also thank Drs. G. A. Shields, D. Hollenbach, R. Rubin, J. Kaler, and A. Natta for helpful discussions, Dr. Benton Ellis for assistance in the data-handling, and the staff of the KAO for their expert operation of this facility. This project was begun while H.L.D. and D.F.L. held National Research Council Associateships at the NASA Ames Research Center. The work at the Ames Research Center was supported by the Astrophysics Division of NASA. We thank Dr. D. E. Osterbrock for granting us observing time at Lick Observatory to make the supplementary optical observations. H.L.D. appreciates the support of the Robert A. Welch Foundation, NSF grant AST 80-20461, and NASA-University of Texas Joint Research Interchange NCA2-OR781-201 during the final stages of this project. D.F.L. received partial support from NASA contract NASW-3159 to the University of Hawaii.

APPENDIX: THE TEMPERATURE FLUCTUATION APPROXIMATION

The case of small temperature variations has been treated by Peimbert (1967), who developed a Taylor-series representation of the temperature-dependent line emissivities and intensity ratios. He defined an average temperature T_0 and a root-mean-square temperature fluctuation parameter t^2 as follows:

$$T_0 = \frac{\int T \; n_i \; n_e \; ds}{\int n_i \; n_e \; ds} \qquad (A - 1)$$

$$t^2 = \frac{\int (T - T_0)^2 \; n_i \; n_e \; ds}{T_0^2 \int n_i \; n_e \; ds} \qquad (A - 2)$$

Any temperature-dependent quantity can then be expanded as a series about the mean temperature, where the second term which is retained involves t^2. For a ratio of two forbidden lines at λ_1 and λ_2 arising from different upper levels, the relationship between the inferred temperature and the average temperature (after Peimbert 1967, equation 15), is:

$$T_{(\lambda_1,\lambda_2)} \cong T_0 \left\{1 + \left(\frac{\chi_1 + \chi_2}{kT_0} - 3\right) \frac{t^2}{2}\right\} \qquad (A - 3)$$

where χ_1 and χ_2 are the excitation energies above ground of the upper levels of transitions 1 and 2 respectively. Substituting the energies for the O III levels, we find:

$$T_{(4363,5007)} = T_0 \left\{1 + \left(\frac{9.13 \times 10^4}{T_0} - 3\right) \frac{t^2}{2}\right\} \qquad (A - 4)$$

and

$$T_{(5007,52\mu)} = T_0 \left\{1 + \left(\frac{2.92 \times 10^4}{T_0} - 3\right) \frac{t^2}{2}\right\} \qquad (A - 5)$$

The behavior at T_0 = 10,000 K is therefore approximately given by:

$$T_{(5007,52\mu)} = T_0 \{1 + .08\ t^2\} \cong T_0 \qquad (A - 6)$$

and

$$T_{(4363,5007)} = T_0 \{1 + 3.07\ t^2\} \cong T_{(5007,52\mu)} \{1 + 3\ t^2\} \qquad (A - 7)$$

Therefore, for $t^2 > 0$, it will always be true that $T_{(4363,5007)} > T_{(5007,52\mu)}$ if temperature fluctuations are the only factor determining the line ratios, and in principle measurements of both temperature indicators will yield values for both T_0 and t^2 in a straightforward way.

TABLE 1

Program Nebulae

Nebula	PK No.	Core Diam. (")	Extinction[a] (c)	F(Hβ)[b] (10^{-10} erg cm^{-2} s^{-1})
NGC 2440	234+02	33	0.63 (1)	1.35 (6)
NGC 3242	261+32	40	0.00 (2,3)	1.58 (6)
NGC 6302	349+01	20	1.22 (4)	8.45 (7)
NGC 6445	008+03	34	0.80 (5)	4.5 (8)
NGC 6543	096+29	18	0.22 (3)	4.67 (8)
NGC 6826	083+12	25	0.03 (3)	1.40 (8)

[a] Logarithmic extinction at Hβ (see text); from references in parentheses.

[b] Integrated nebular Hβ fluxes, where observed values have been corrected for extinction using the value of c in the previous column.

References:

(1) Shields et al. 1981.

(2) Barker 1979.

(3) Aller and Czyzak 1983.

(4) Aller et al. 1981.

(5) Aller et al. 1973.

(6) Carrasco, Serrano, and Costero 1983.

(7) Calculated from the radio flux $S_{5\ GHZ}$ = 3.49 Jy of Milne and Aller (1975), assuming T_e = 20,000 K and given value of c.

(8) This work.

TABLE 2

Measured Line Fluxes

Nebula	F (52 μm)	F (88 μm)	F (5007 Å)[a]	$\log \frac{F(5007\ Å)}{F(4363\ Å)}$[a]
		(10^{-10} erg cm^{-2} s^{-1})		
NGC 2440	1.72±0.24	0.48±0.10	19.4±2.9 (1)	1.75 (4)
NGC 3242	4.41±0.40	1.63±0.24	19.2±1.9 (1)	2.02 (5,6)
NGC 6302	0.73±0.18	-	115±28 (2)	1.50 (2)
NGC 6445	-	< 0.2 (3σ)	6.4±1.6 (3)	1.78 (7)
NGC 6543	8.79±0.97	1.10±0.20	27.0±4.0 (3)	2.56 (8)
NGC 6826	3.66±0.44	0.96±0.22	9.2±0.9 (3)	2.40 (8)

[a]Flux or flux ratio corrected for extinction assuming the extinction law of Miller and Mathews (1972) and the values of c given in Table 1. Sources of the uncorrected fluxes are indicated in parentheses.

References:

(1) From 4959 Å/Hβ ratio of Kaler 1976.

(2) Danziger, Frogel, and Persson 1973.

(3) This work.

(4) Shields et al. 1981.

(5) Barker 1978.

(6) Aller and Czyzak 1979.

(7) Aller et al. 1973.

(8) Bohuski, Dufour, and Osterbrock 1974.

TABLE 3

Derived Physical Parameters

Nebula	log n_e(O III) (cm^{-3})	log n_e(O II) (cm^{-3})	$T_e\left(\frac{5007\ Å}{52\ \mu m}\right)$ (°K)	$T_e\left(\frac{4363\ Å}{5007\ Å}\right)$ (°K)	t^2
NGC 2440	3.2±0.2	3.2 (1)	13,000±1400	14,300	.025
NGC 3242	3.0±0.1	3.3 (2)	9,800± 500	11,500	.058
NGC 6302	4.3[a]	3.8 (1)	--	19,000	--
NGC 6445	> 3.0[b]	2.9 (1)	--	14,000	--
NGC 6543	$4.0\ ^{+\infty}_{-0.4}$ [c]	3.6 (3)	5,800± 300	8,000	.126
NGC 6826	3.2±0.2	3.2 (3)	7,700± 400	8,800	.048

[a]Derived from F(5007 Å)/F(52 μm) assuming T_e(4363 Å/5007 Å).

[b]Derived from F(5007 Å) and limit on 88 μm line, assuming T_e(4363 Å/5007 Å).

[c]The upper range of the line ratio corresponds to an unphysical value, beyond the high-density limit (see Figure 3).

References:

(1) Aller and Epps 1976; n_e determined from their values of x assuming T_e = T (5007 Å/52 μm) from column 4.

(2) Barker 1978.

(3) Lutz 1974, corrected for temperature dependence to T_e in column 4.

REFERENCES

Aggarwal, K.M. 1983, Ap. J. Suppl., 52, 387.

Aggarwal, K.M., Baluja, K.L., and Tully, J.A. 1982, Mon. Not. Roy. Astr. Soc., 201, 923.

Aller, L.H., and Czyzak, S.J. 1979, Astrophys. Space Sci., 62, 397.

Aller, L.H., and Czyzak, S.J. 1983, Ap. J. Suppl., 51, 211.

Aller, L.H., Czyzak, S.J., Craine, E., and Kaler, J.B. 1973, Ap. J., 182, 509.

Aller, L.H., and Epps, H.W. 1976, Ap. J., 204, 445.

Aller, L.H., Ross, J.E., O'Mara, B.J., and Keyes, C.D. 1981, Mon. Not. Roy. Astr. Soc., 197, 95.

Baluja, K.L., and Doyle, J.G. 1981, J. Phys. B: At. Mol. Phys., 14, L11.

Barker, T. 1978, Ap. J., 219, 914.

Barker, T. 1979, Ap. J., 227, 863.

Bignell, R.C. 1983, in IAU Symposium 103, Planetary Nebulae, ed. D. Flower(Dordrecht: Reidel) , p. 69.

Bohuski, T.J., Dufour, R.J., and Osterbrock, D.E. 1974, Ap. J., 188, 529.

Bond, H.E. 1981, Pub. Astr. Soc. Pac., 93, 429.

Carrasco, L., Serrano, A., and Costero, R. 1983, Rev. Mex. Astron. Astrof., 8, 187.

Czyzak, S.J., Aller, L.H., and Kaler, J.B. 1968, Ap. J., 154, 543.

Danziger, I.J., Frogel, J.A., and Persson, S.E. 1973, Ap. J. (Lett.), 184, L29.

Dinerstein, H.L. 1983, in IAU Symposium 103, Planetary Nebulae, ed. D. Flower(Dordrecht: Reidel) , p. 79.

Eissner, W., Seaton, M. J. 1974, J. Phys. B: Atom. Molec. Phys., 7, 2533.

Gatley, I., Becklin, E.E., Werner, M.W., and Wynn-Williams, C.G. 1977, Ap. J., 216, 277.

Haas, M.R., Erickson, E.F., McKibbin, D.D., Goorvitch, D., and Caroff, L.J. 1982, Icarus, 51, 476.

Hayes, D.S. 1970, Ap. J., 159, 165.

Hayes, D.S., and Latham, D.W. 1975, Ap. J., 197, 593.

Huggins, W. 1864, Proc. Roy. Soc. London, A, 13, 492.

Hyland, A.R., McGregor, P.J., Robinson, G., Thomas, J.A., Becklin, E.E., Gatley, I., and Werner, M.W. 1980, Ap. J., 241, 709.

Kaler, J.B. 1974, Astron. J., 79, 594.

Kaler, J.B. 1976, Ap. J., 210, 113.

Kaler, J.B. 1980, Ap. J., 239, 78.

Lambert, D. L. 1978, Mon. Not. Roy. Astr. Soc., 182, 249.

Lester, D.F. et al. 1984a, in preparation.

Lester, D.F., and Dinerstein, H.L. 1984, Ap. J. (Letters), in press.

Lester, D.F., Dinerstein, H.L., Werner, M.W., and Harvey, P. 1984b, submitted to Ap. J..

Lester, D.F., Dinerstein, H.L., Werner, M.W., Watson, D.M., and Genzel, R.L. 1983, Ap. J., 271, 618.

Lutz, J.H. 1974, Pub. Astr. Soc. Pac., 86, 888.

Melnick, G., Gull, G. E., and Harwit, M. 1979, Ap. J. (Letters), 227, L35.

Melnick, G., Russell, R.W., Gull, G.E., and Harwit, M. 1981, Ap. J., 243, 170.

Mendoza, C. 1983, in IAU Symposium 103, Planetary Nebulae, ed. D. Flower(Dordrecht: Reidel) , p. 143.

Mihalszki, J.S., and Ferland, G.J. 1983, Pub. Astr. Soc. Pac., 95, 284.

Miller, J.S., and Mathews, W.G. 1972, Ap. J., 172, 593.

Millikan, A.G. 1974, Astron. J., 79, 1259.

Milne, D.K., and Aller, L.H. 1975, Astr. Ap., 38, 183.

Minkowski, R. 1964, Pub. Astr. Soc. Pac., 76, 197.

Moorwood, A.F.M., Baluteau, J.-P., Anderegg, M., Coron, N., Biraud, Y., and Fitton, B. 1980, Ap. J., 238, 565.

Moseley, H. 1980, Ap. J., 238, 892.

Moseley, H., and Silverberg, R.F. 1981, Bull. AAS, 13, 519.

Nussbaumer, H., and Storey, P.J. 1981, Astr. Ap., 99, 177.

Peimbert, M. 1967, Ap. J., 150, 825.

Peimbert, M. 1971, Bol. Obs. Ton. y Tacu., 6, 29.

Peimbert, M., and Costero, R. 1969, Bol. Obs. Tonantzintla y Tacubaya, 5, 3.

Perinotto, M. 1983, in IAU Symposium 103, Planetary Nebulae, ed. D. Flower(Dordrecht: Reidel) , p. 323.

Pottasch, S.R. 1984, Planetary Nebulae: A Study of Late Stages of Stellar Evolution (Dordrecht: Reidel), p. 10.

Reay, N.K., and Worswick, S.P. 1982, Mon. Not. Roy. Astr. Soc., 199, 581.

Rubin, R.H. 1969, Ap. J., 155, 841.

Saraph, H.E., Seaton, M.J., and Shemming. J. 1969, Phil. Trans. Roy. Soc. London, A, 264, 77.

Shields, G.A., Aller, L.H., Keyes, C.D., and Czyzak, S.J. 1981, Ap. J., 248, 569.

Shields, G.A., Dalgarno, A., and Sternberg, A. 1983, Phys. Rev. A., 28, 2137.

Simpson, J.P. 1975, Astr. Ap., 39, 43.

Simpson, J.P., Cuzzi, J.N., Erickson, E.F., Strecker, D.W., and Tokunaga, A.T. 1981, Icarus, 48, 230.

Storey, J.W.V., Watson, D.M., and Townes, C.H. 1980, Internat. J. Infr. Mil. Waves, 1, 15.

Torres-Peimbert, S., and Peimbert, M. 1977, Rev. Mex. Astr. Ap., 2, 181.

Wampler, E. J. 1966, Ap. J., 144, 921.

Ward, D.B., Dennison, B., Gull, G., and Harwit, M. 1975, Ap. J. (Letters), 202, L31.

Watson, D.M. 1982, Ph.D. thesis, University of California at Berkeley.

Watson, D.M., and Storey, J.W.V. 1980, Internat. J. Infr. Mil. Waves, 1, 609.

Watson, D.M., Storey, J.W.V., Townes, C.H., and Haller, E.E. 1981, Ap. J., 250, 605.

Welty, D.E. 1983, Pub. Astr. Soc. Pac., 95, 217.

Werner, M.W., Gatley, I., Harper, D.A., Becklin, E.E., Lowenstein, R.F., Telesco, C.M., an Thronson, H.A. 1976, Ap. J., 204, 420.

FIGURE CAPTIONS

Figure 1. - The energy level diagram for the ground term of the O^{++} ion is shown. The optical transitions are identified at left, while the fine-structure levels and transitions are indicated on an expanded scale at right.

Figure 2. - This figure shows representative spectra of the 52 μm and 88 μm [O III] fine-structure lines. These spectra are presented in order to illustrate the quality of the data; flux scales and dispersions are not uniform. At top are displayed measurements of NGC 6543, obtained in June 1982 (52 μm) and July 1981 (88 μm). Both lines of NGC 3242 (at bottom) were observed in May 1983 and have a higher signal-to-noise ratio due to the improved instrumental sensitivity. The data were averaged over bins much smaller than the instrumental resolution (represented by the observed line width) and fitted with Lorentzian profiles in order to derive total line intensities. The line fluxes and statistical uncertainties are given in Table 2.

Figure 3. - The normalized volume emissivity (left axis) of the 52 μm [O III] line is plotted as a function of density and temperature. The main variation is the decrease with density n_e above the critical density of 3 x 10^3 cm^{-3}. The curves correspond to three values of the temperature that bracket the range of interest. Also shown is the behavior of the density diagnostic ratio (52/88 μm) for the same range of physical conditions.

These emissivities incorporate recent improved values for the collision strengths and A values of the fine-structure transitions (see Section IIIA).

Figure 4. - The [O III] temperature-density plane defined by the set of lines 5007 Å, 52 μm, and 88 μm is presented (see Section IIIB). The grid gives calculated line intensity ratios for a range of values of log n_e, T_e. Four planetary nebulae for which both far-infrared [O III] lines were observed (see Table 2) are located in this plane, with error bars indicating the uncertainties in the line ratios and in the deduced physical properties.

AUTHOR'S ADDRESSES

HARRIET L. DINERSTEIN and DANIEL F. LESTER: Astronomy Department, The University of Texas at Austin, Austin, Texas 78712

MICHAEL W. WERNER: Mail Stop 245-6, NASA Ames Research Center, Moffett Field, California 94035

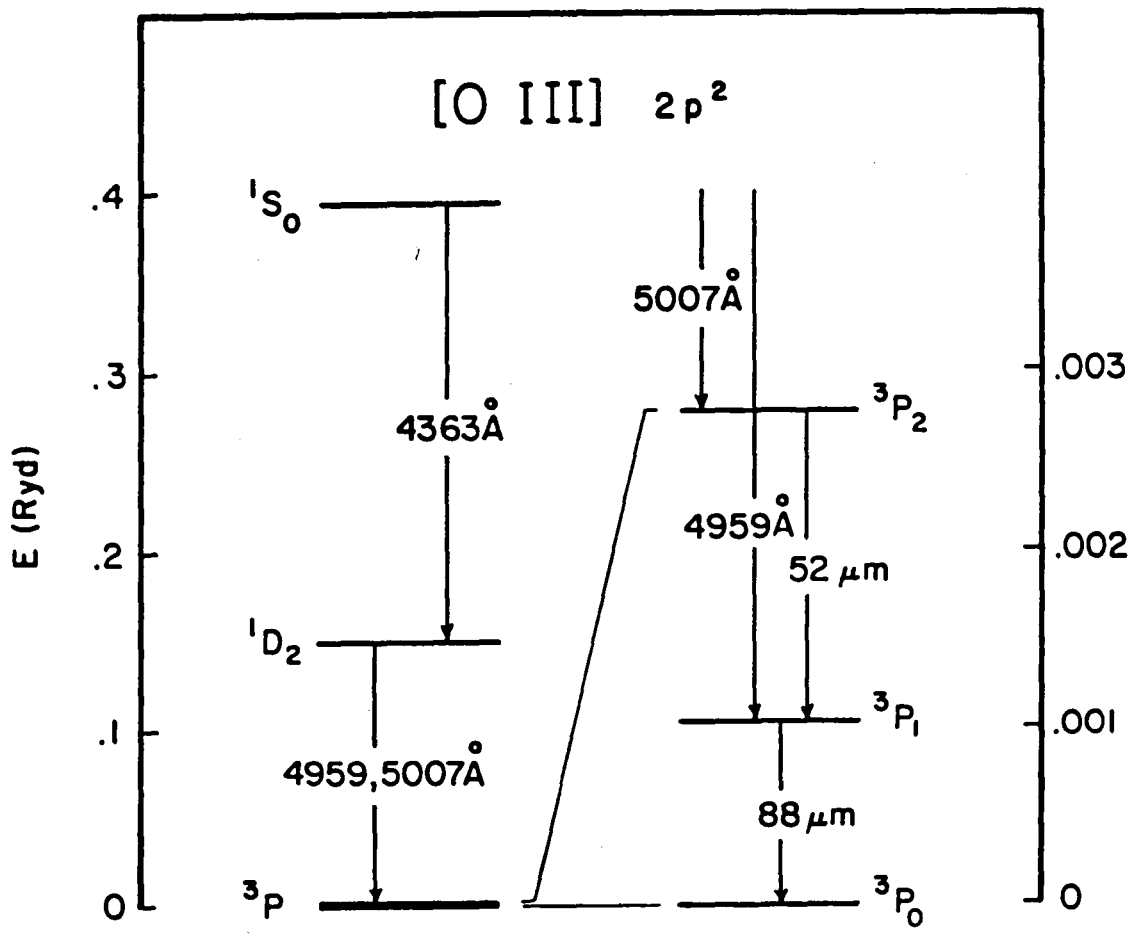
[O III] 2p²
E (Ryd)
.4
.3
.2
.1
0
.003
.002
.001
0
¹S₀
¹D₂
³P
³P₂
³P₁
³P₀
4363Å
4959,5007Å
5007Å
4959Å
52 μm
88 μm

Fig. 1

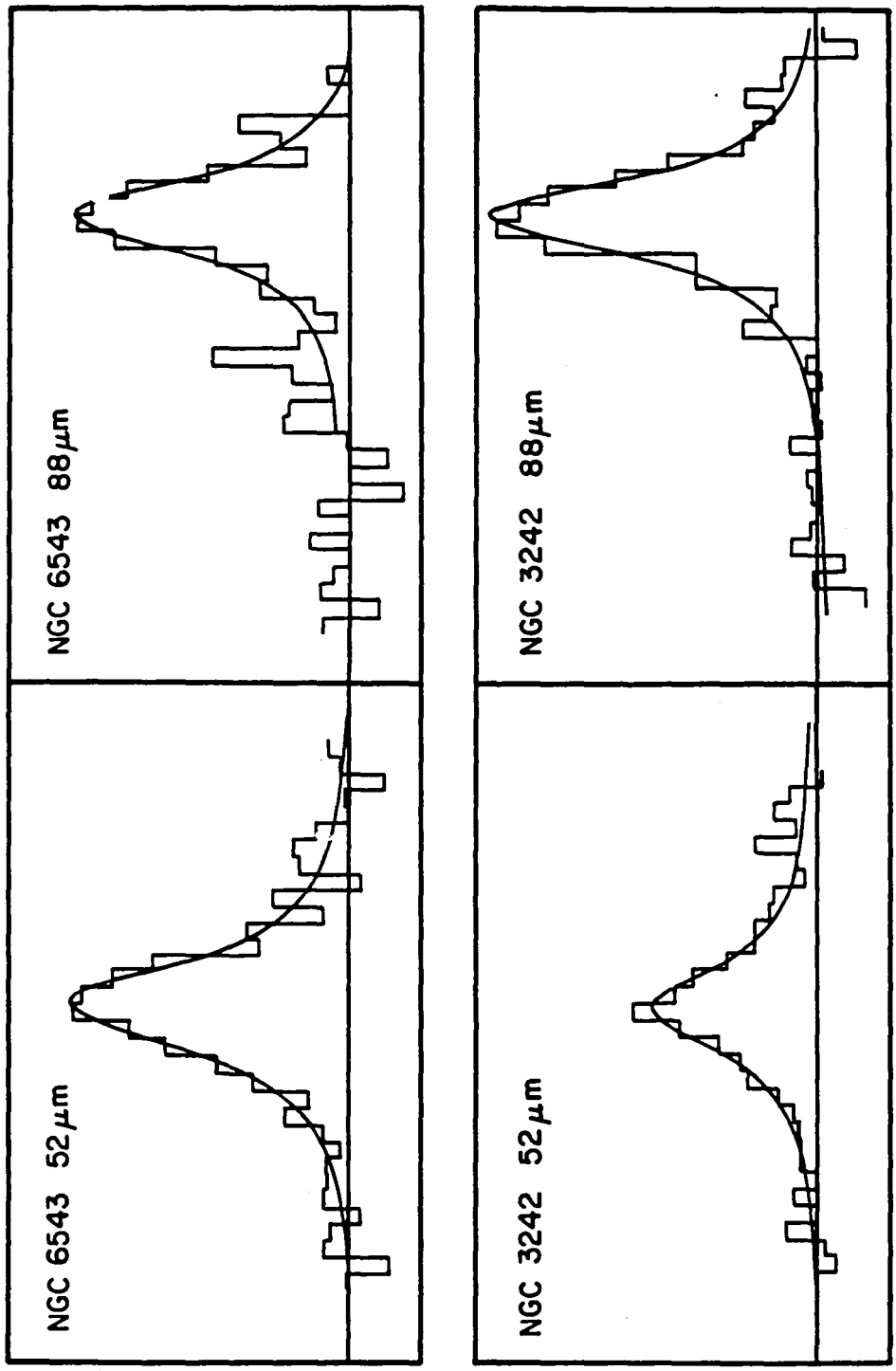

Fig. 2

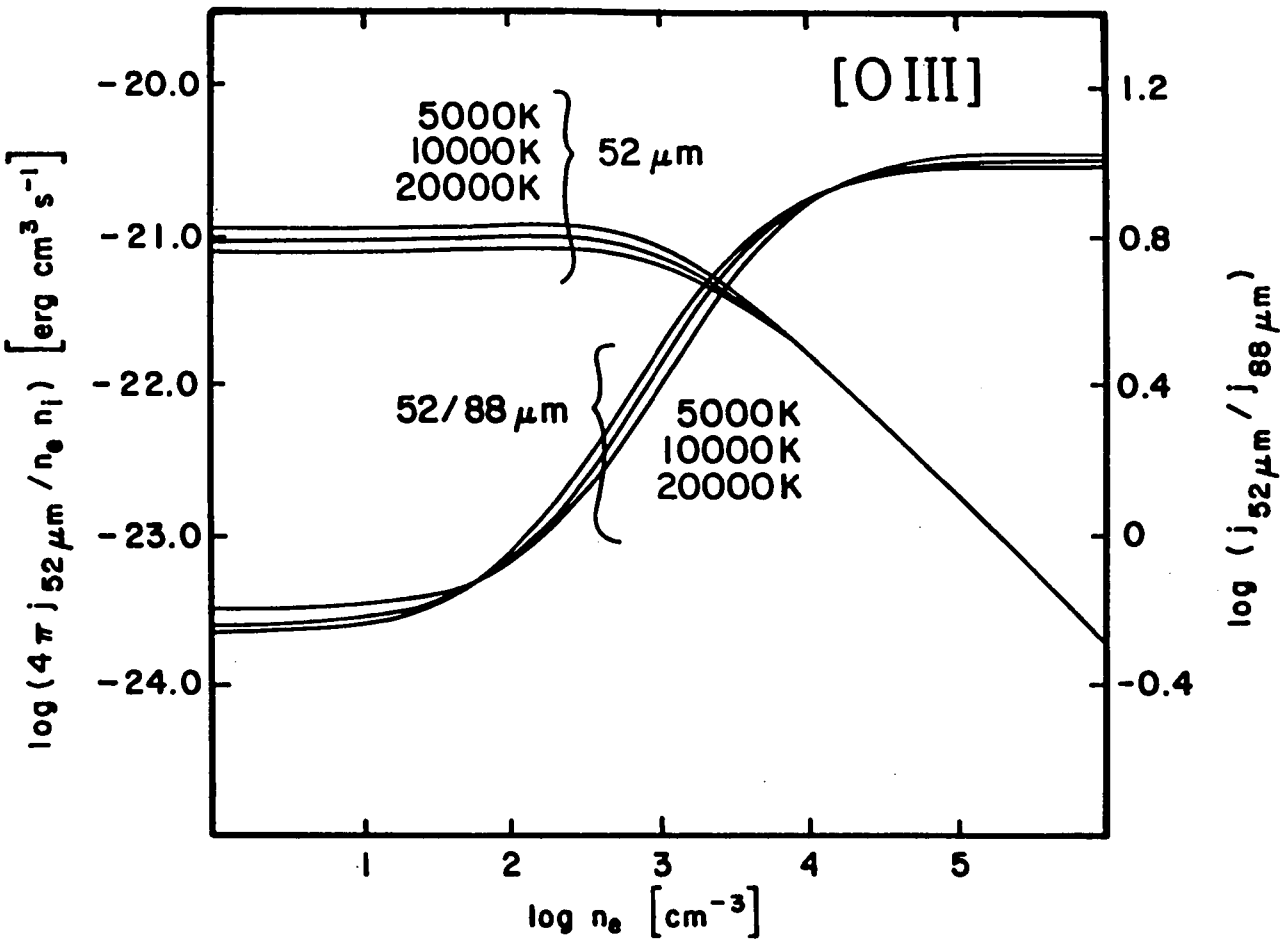
[O III]
5000K
10000K
20000K
52 μm
52/88 μm
5000K
10000K
20000K
-20.0
-21.0
-22.0
-23.0
-24.0
1.2
0.8
0.4
0
-0.4
1
2
3
4
5
log (4π j52μm / ne ni) [erg cm3 s-1]
log (j52μm / j88μm)
log ne [cm-3]

Fig. 3

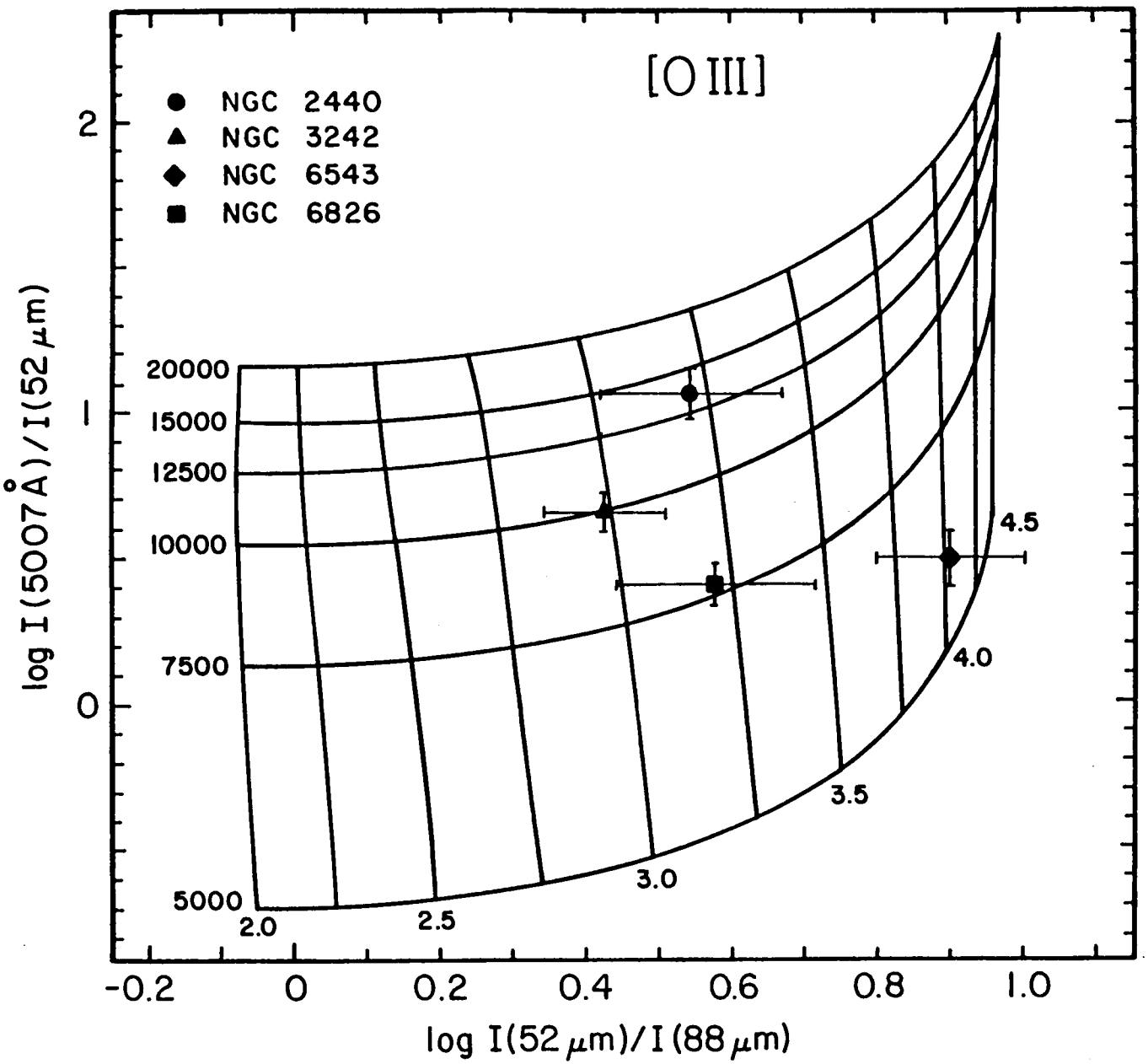
[O III]
NGC 2440
NGC 3242
NGC 6543
NGC 6826
log I(5007Å)/I(52 μm)
log I(52 μm)/I(88 μm)
20000
15000
12500
10000
7500
5000
2.0
2.5
3.0
3.5
4.0
4.5
-0.2
0
0.2
0.4
0.6
0.8
1.0
2
1
0

Fig. 4

1. Report No.	2. Government Accession No.	3. Recipient's Catalog No.
NASA TM-86670		

4. Title and Subtitle	5. Report Date
FAR-INFRARED LINE OBSERVATIONS OF PLANETARY NEBULAE: I. THE [O III] SPECTRUM	February 1985
	6. Performing Organization Code
7. Author(s)	8. Performing Organization Report No.
Harriet L. Dinerstein,* Daniel F. Lester,* and Michael W. Werner†	85091
	10. Work Unit No.
9. Performing Organization Name and Address	
*University of Texas at Austin, Austin, TX 78712 †Ames Research Center, Moffett Field, CA 94035	11. Contract or Grant No.
	13. Type of Report and Period Covered
12. Sponsoring Agency Name and Address	Technical Memorandum
National Aeronautics and Space Administration Washington, DC 20546	14. Sponsoring Agency Code 352-02-03

15. Supplementary Notes
Preprint Series #26. Supported by NASA grants.
Point of Contact: L. C. Haughney, Ames Research Center, MS 211-12, Moffett Field, CA 94035, (415) 694-5339 or FTS 464-5339

16. Abstract

Observations of the far-infrared fine-structure lines of [O III] have been obtained for six planetary nebulae. The infrared measurements are combined with optical [O III] line fluxes to probe physical conditions in the gas. From the observed line intensity ratios, we obtain a simultaneous solution for electron temperature and density, as well as a means of evaluating the importance of inhomogeneities. Densities determined from the far-infrared [O III] lines agree well with density diagnostics from other ions, indicating a fairly homogeneous density in the emitting gas. Temperatures are determined separately from the [O III] 4363/5007 Å and 5007 Å/52 μm intensity ratios and compared. Systematically higher values are derived from the former ratio, which is expected from a nebula which is not isothermal. Allowance for the presence of temperature variations within these nebulae raises their derived oxygen abundances, which may allow us to reconcile nebular oxygen abundance determinations with the solar value.

17. Key Words (Suggested by Author(s))	18. Distribution Statement
Nebulae: planetary Nebulae: abundances Infrared: spectra	Unlimited Subject category - 89

19. Security Classif. (of this report)	20. Security Classif. (of this page)	21. No. of Pages	22. Price*
Unclassified	Unclassified	43	A03

*For sale by the National Technical Information Service, Springfield, Virginia 22161

End of Document